Wisetjindawat, W., Wilson, E., Bullock, S., & Espinosa Mireles De Villafranca, A. (2019). Modeling the Impact of Spatial Correlations of Road Failures on Travel Times during Adverse Weather Conditions. *Transportation Research Record: Journal of the Transportation Research Board*, *2019*, 1-12. https://doi.org/10.1177/0361198119844251

Modelling the Impact of Spatial Correlations of Road Failures on Travel Times during Adverse Weather Conditions

Authors:

Wisinee Wisetjindawat (Corresponding Author)
Department of Engineering Mathematics, University of Bristol
Merchant Venturers Building, Woodland Road, Clifton
Bristol, BS8 1UB
Tel: +44-117-985-8792
Email: w.wisetjindawat@bristol.ac.uk

R. Eddie Wilson
Department of Engineering Mathematics, University of Bristol
Merchant Venturers Building, Woodland Road, Clifton
Bristol, BS8 1UB
Email: re.wilson@bristol.ac.uk

Seth Bullock
Department of Computer Science, University of Bristol
Merchant Venturers Building, Woodland Road, Clifton
Bristol, BS8 1UB
Email: seth.bullock@bristol.ac.uk

Alonso Espinosa Mireles de Villafranca
Department of Engineering Mathematics, University of Bristol
Merchant Venturers Building, Woodland Road, Clifton
Bristol, BS8 1UB
Email: alonso.espinosa@bristol.ac.uk

Submission Date: 1st August 2018
Resubmission Date: 15th November 2018
Paper Number: 19-04126
Word Count: Text (6,444) + Tables (4*250) = 7,444
98th Annual Meeting of the Transportation Research Board, January 13-17, 2019

ABSTRACT

Traveling in extreme adverse weather involves a high risk of travel delay and traffic accidents. There is a need to assess the impact of extreme weather on transport infrastructure and to find suitable mitigation strategies to alleviate the associated undesirable outcomes. Previous work in vulnerability studies applied either a constant failure probability or an assumed probabilistic distribution. Such assumptions ignored many factors causing the occurrence of road failure, especially that infrastructure components tend to fail interdependently. Based on empirical data of road failures and rainfall intensity during a typhoon, this study develops a statistical model, incorporating spatial correlations among the segments of road infrastructure, and uses it to evaluate the impact of the typhoon on travel time reliability. Mixed effects logistic regression as well as rare events logistic regression are applied to understand the factors involved in road failures and the spatial correlations of the failed segments. The analysis suggested that, in addition to the rainfall intensity, the road geometry, including elevation, land slope and distance from the nearest river, were important factors in the failure. In addition, there is a significant correlation of failures within watersheds. This model gives an insight into the characteristics of road failures and their associated travel risks, which is useful for authorities to find proper mitigations to reduce the adverse effects in future disasters.

Keywords: Transport Resilience, Typhoon, Travel Time Reliability, Spatial Correlations

INTRODUCTION

An extreme adverse weather event can cause significant travel disruption and thereby have consequences for the economy as a whole. Heavy rain may result in flooding, landslides, and weaken the structure of road foundations, bridges and tunnels, resulting in reduced road capacity. These problems not only reduce the speed of travel but also impose delays, since driving under extreme weather conditions involves a higher risk of accidents due the degraded road condition, reduced visibility and extended braking distances.

Understanding how mitigation strategies are influenced by interdependencies between infrastructure components should help achieve better whole system resilience during such extreme events. Multiple infrastructure components may tend to fail in an interdependent fashion as a result of their vulnerability to a common cause. For example, during a typhoon, a river surge is often one of the primary causes of road failure. Flood water from upstream flows into and subsequently floods the river basin downstream. Hence, road segments along the same stretch of river fail from surface flooding and surge water at the same time. Moreover, a failure of one infrastructure component may trigger a series of failures in other components. For example, the increased risk of traffic accidents on a congested stretch of road affected by bad weather may lead to an increased risk of traffic accidents on adjacent stretches of road if congestion spreads. In either case, the failure of infrastructure components may be correlated. However, previous works in vulnerability studies applied either a constant failure probability or an assumed probabilistic distribution. These methods do not consider how the interdependencies impact on the modelling. Thus, modelling system failure by assuming that each component fails independently is likely to lead to unrealistic outcomes.

In order to develop an improved prediction methodology, this study aims to incorporate spatial correlations among the segments of a road infrastructure into a model of the impact of typhoons on road conditions and travel time reliability. Using a statistical method, two types of model, with and without correlated failure for segments within the same watershed, are developed and compared. The models are calibrated using data on road failures, geometric characteristics and rainfall intensities during Typhoon Roke in the Tokai region, Japan. The calibrated failure model of road segments then informs the probability of road segment failure and is used as an input into the measurement of travel time reliability between a given origin and destination during a typhoon. This method not only improves the prediction of the impact of the typhoon, but vulnerable locations can also be identified. These results give a better understanding of the extent of the impact of extreme weather which may help the authorities identify effective mitigation strategies.

In the next section, the literature related to this study is provided. Later, the mathematical models are explained. Then we provide and discuss the calibration models described above. Finally, the findings and recommendations are drawn from this study to improve the future research.

LITERATURE REVIEW

Vulnerability studies stem from reliability studies, which during 1990s focused mainly on travel time reliability on congested road networks and the probability that a network will deliver a required standard of performance *(1)*. Over the last two decades, vulnerability studies emerged and received intense attention from numerous researchers around the world *(2)*. Both studies have different approaches to the problem. Reliability studies focus on the reliability of transport systems, considering uncertainties that cause travel time fluctuations. Uncertainties are from demand and supply sides, such as seasonal demand fluctuations and incidents and accidents that occurred along a network and caused reduction in road capacity *(3)*. On the other hand, vulnerability studies focus on identifying the critical segments of a transport network in order to inform mitigation strategies *(4)*. Vulnerability studies were motivated by a growing number of natural and manmade disasters, creating a level of disruption far beyond that of daily congestion.

In reliability studies, there are three methods of measuring the performance of a transport network: terminal reliability, travel time reliability, and capacity reliability. Terminal reliability, sometimes called connectivity reliability, is the earliest approach, originating with Iida and Wakabayashi *(5)*. Terminal reliability measures the probability that a given Origin/Destination (OD) pair remains connected in a network. A network will be considered successful if at least one path that connects the OD pair is operational. However, this measurement ignores the additional congestion from the increment in travel demand on the remaining operable paths. Hence, travel time reliability takes into account the consequent congestion. This reliability measurement considers the probability that a trip between a given OD pair can be completed successfully within a specific time interval. Travel time reliability is the most common method used to evaluate network performance for normal daily congestion *(6)*. However, during an extreme event, a network can be largely degraded and the travel time between an OD pair might increase significantly. Thus, another measurement proposed by Asakura *(7)* formulates the probability as a ratio of travel times between affected and normal conditions. Later, Chen et al *(6, 8)* introduced capacity reliability to evaluate the performance of a degradable road network. The travel time is compared between two states: with degraded and non-degraded capacities. Capacity reliability is defined as the probability that the reserve capacity of the network is greater than or equal to the required demand for a given capacity loss due to degradation.

Once again, unlike reliability studies, vulnerability studies mainly focus on the identification of critical segments in a transport network. Vulnerability studies are categorized into four main groups: inventory-based risk assessment; topology-based analysis; accessibility-based analysis, and serviceability-based analysis *(1)*. The risk assessment considers the state of operation of individual components in a network due to the effects of internal and external factors and defines the associated risks. The topology-based approach identifies critical locations in a network based on the effects of their failure on the reduction in network connectivity, such as the works of Kermanshah and Derrible *(9)* and Berche et al *(10)*. However, this category focuses on the connectivity and ignores the aspect of travel demand. Most vulnerability studies used an accessibility-based approach, which measures the loss in accessibility when one or more segments of a network failed. The consequent accessibility losses were addressed in various units, such as travel cost increment in Jenelius et al. *(11)* and socio-economic impact in Taylor et al. *(12, 13)*. However, accessibility approach vulnerability studies do not account for simultaneous failure of multiple road segments. In most works, the simulation is performed by closing each link one by one and measuring the changes in accessibility. On the other hand, the serviceability-based approach analyzes the capability of a transport network to meet certain functional requirements when the network is degraded, such as the works in Sumalee and Kurauchi *(14),* Haghighi et al *(15),* Asadabadi and Miller-Hooks *(16),* and Wisetjindawat et al. *(17, 18)*.

Among the serviceability approaches, most works apply a constant failure probability (in *(14*, *15)*) or use a probability distribution (in (*16, 17, 18)*). In the works of *(17)* and *(18)*, their approach used a stochastic method by assuming a probability function to explain the occurrences of road failure due to a natural disaster. The link failure probability was assumed to follow a negative exponential distribution with a given failure rate derived from a climate data. Using this probability distribution, however, important factors, such as road geometry and surrounding environment, are not taken into consideration. In addition, the failure model assumed independent failure of each road link. In fact, there are correlations among the failed segments, as explained by flooded roads in the same floodplain. On the other hand, the work of *(16)* considered the locations of road elements and elevations in their failure during storms and the consequent impacts on the road network. However, it was formulated as an optimization problem and hence it becomes difficult to apply to a larger network due to computational burden. Thanks to the availability of geometry data, the failure records, and the actual typhoon intensity, this study adopts a statistical model and integrates the spatial correlation of the failure of road segments, as well as the geometric characteristics of the region, into the modeling to improve the predictive accuracy and the proposed method can be applied to a large-scale road network.

The statistical analysis event distributions, using logistic regression, has gained attention in recent years. However, in the field of natural hazards, often the datasets are not approximately equal between groups (e.g., the number of road segments that fail during a typhoon may be small by comparison with the total number of road segments being considered), resulting in problems in predictive accuracy towards the minority *(19)*. When the occurrence of an event type is very rare, such as one or two percent, the model often has a strong bias towards the majority. For example, a seemingly good model with a 99 percent hit ratio often underestimates the occurrence of the minority event type. A logistic regression model for rare event data, or the so called rare-logit, was proposed by King and Zeng *(20, 21)* to deal with imbalanced binary data when one option is a dozen or even a thousand times less frequent than the other. Originally, the work was applied to predict political conflicts in pairs of countries at war each year since WW2, where the conflict percentage was only 0.34%, as normal logistic regression struggles with such tiny fractions. Many works on logistic regression for imbalanced datasets can be found, especially for applications in natural hazards, such as in Guns and Vanacker *(19)* and Bai et al. *(22).* In this study, a similar problem occurred since only approximately 5% of the road segments failed due to the 2011 typhoon Roke. Without a method for correction, the failed segments are difficult to predict accurately using a normal logistic regression. The rare-logit technique for estimating rare events is hence adopted in this study.

METHODOLOGY

The model framework is as depicted in Figure 1. GIS maps of the rainfall intensity of the typhoon, the geometry of the region, rivers, and water system are used to calibrate the failure probability of each road segment. These maps are projected into a 100×100 m^2 grids of the road system of the Tokai region. Two models are compared with and without spatial correlations. The calibrated models are used to predict the failures of road segments which later determines the failures of road links. Next, a stochastic model, like one presented in *(17, 18),* is used to determine travel conditions during the disaster.

A Monte Carlo simulation is adopted to identify links impacted by the typhoon using the failure probability described in the next section. Based on the work by Hoghighi et al *(15)*, we assume three failure stages of the affected links: moderate, extensive, and completely nonoperational. We again assigned the failure stage using Monte Carlo simulation. The characteristics of the affected links, including capacity and free flow speed, are reduced according to the failure stage. A set of deteriorated road networks with random failure stages is generated up to a preset number (i.e., maximum iteration). At each step, one of the generated road networks is used as an input into traffic assignment, together with the travel demand OD. This step repeats until all the generated road networks are used. The final results on the travel condition, such as link volume, traverse time etc., can be obtained and later used to derive the travel time reliability.

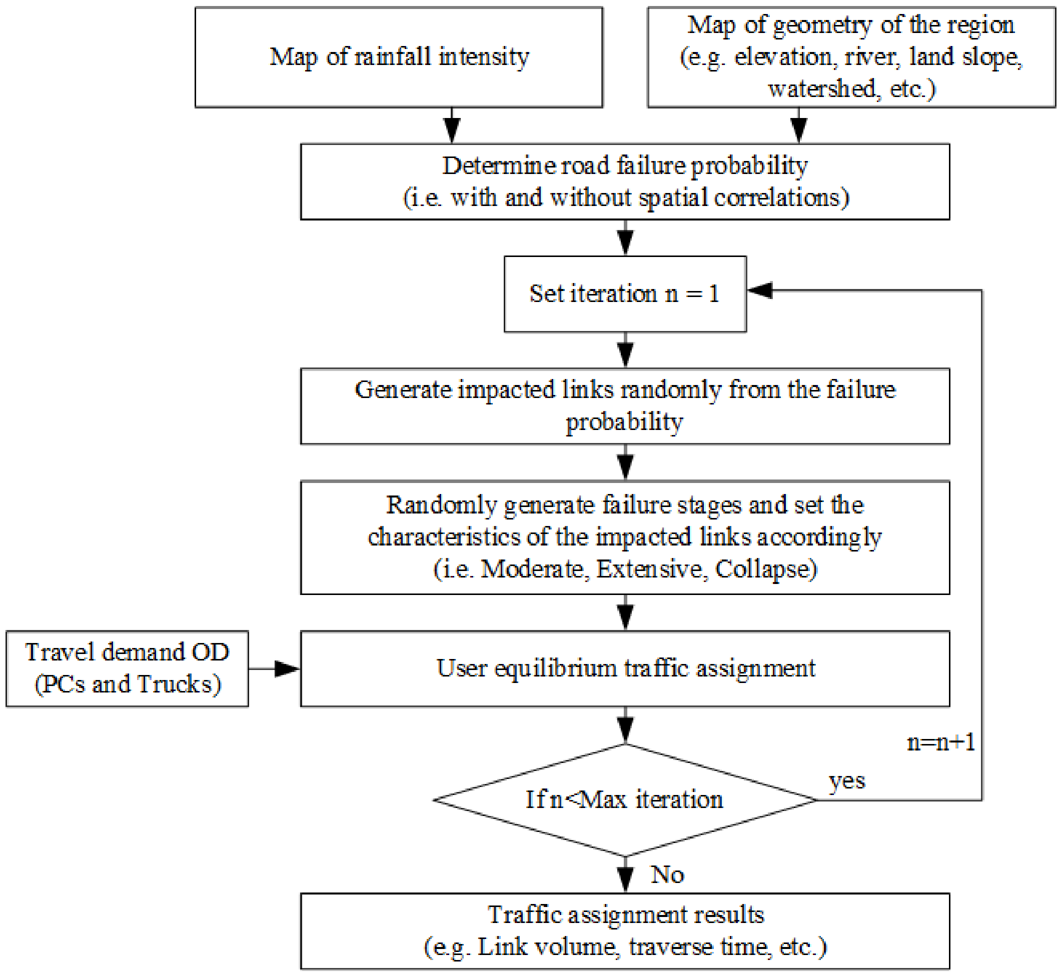

FIGURE 1 Analysis framework

Incorporating Spatial Correlations among Road Segments into the Failure Model

Mixed effects logistic regression (MELR), which is another form of Generalized Linear Mixed Model (GLMM), is often used to predict discrete outcomes when observations are correlated. This technique has been applied widely across different fields, such as medicine *(23)*, residential choice *(24)* and so on. In many cases, observations are found having some kind of clustering and tendency to be correlated within clusters *(25)*. In our context, the road failures can be viewed as spatially correlated according to their clusters (i.e., floodplain where the road segment locates). In other words, multiple components in the same floodplain normally fail together.

Mathematically, GLMM includes both fixed and random effects (hence, it is called a mixed model) and the structure of the correlation can be specified in the disturbance part. Due to its flexible structure, the disturbance part can be designed to include various forms, such as, spatial and/or temporal correlations, cluster effects, and other types of correlation structures. The observed outcomes can be in any form: discrete or continuous. GLMM has the general form

$$\boldsymbol{y} = \boldsymbol{X\beta} + \boldsymbol{Zu} + \boldsymbol{\varepsilon} \tag{1}$$

where $\boldsymbol{y}$ is a [N×1] vector of observed outcomes and N is the number of observations, $\boldsymbol{X}$ is a [N×K] vector of k explanatory variables. Further, $\boldsymbol{\beta}$ is a [K×1] vector of fixed-effects regression coefficients, $\boldsymbol{Z}$ is a [N×Q] design matrix for the Q random effects to specify the correlation structure, $\boldsymbol{u}$ is a [Q×1] vector of the random effect coefficients with mean 0 and variance-covariance Σ, and $\boldsymbol{\varepsilon}$ is a [N×1] vector of random variables that are not explained by the model.

When GLMM takes the form of logistic regression with binary outcomes for clustered data, the formulation of the binary MELR becomes as shown in Equation (2). Here $\boldsymbol{y}$ represents the probability of occurrence, which is specified in terms of log-odds (in the left side of Equation (2)), of the probability that road segment i, which belongs to cluster j, has either failed (y_{ij} =1) or survives (y_{ij} =0).

$$logit\left(\frac{\Pr(y_{ij}=1)}{1-\Pr(y_{ij}=1)}\right) = \boldsymbol{X}_{ij}\boldsymbol{\beta} + \boldsymbol{v}_j, \qquad i = 1,2,\ldots,N; j = 1,2,\ldots,Q \tag{2}$$

Here $\boldsymbol{X}_{ij}$ is a [1×K] vector of k explanatory variables for the failure of segment i of cluster j and $\boldsymbol{v}_j$ is the random effect from cluster j, obtained from $\boldsymbol{Zu}$.

This study applies MELR for cluster effects where the road segments are clustered into different watersheds. The effect of correlations of segments within the same watershed are incorporated in the designed disturbance part ($\boldsymbol{Zu}$). In this case, the number of watersheds is 130, hence the size of the designed correlation matrix $\boldsymbol{Z}$ becomes [N×130], where N is the total number of road segments in the study area.

Rare Events Logistic Regression for Predicting Road Failures

Failure of segments in an infrastructure by natural hazards is considered to be a rare event. In practice, only a small percentage of failures can be found. This section describes the method used to reduce the estimation bias that occurred by applying logistic regression to an imbalanced dataset.

King and Zeng *(20, 21)* proposed a rare events logit model, using a Monte Carlo simulation to make a biased dataset and later applying a method to fix the bias due to the random simulation. However, attention should be paid in preparing a bias dataset for the estimation. In the case of a rare travel mode choice, it might be possible to collect a number of rare samples during the data collection stage. However, this method cannot be applied in case of natural hazards, when the number of failed segments is fixed. Chawla *(26)* classified sampling techniques used for balancing imbalanced datasets into two categories: over and under samplings. Under-sampling the majority category and over-sampling the minority category ensures that the approximate same number of randomly selected cases are considered from each category. However, Chawla *(26)* noted that both methods have short-comings; the under-sampling can potentially remove certain important samples, while over-sampling can lead to an overfitting problem on the multiple copies of the minority. The overfitting problem happens when a model describes the errors instead of the underlying relationship.

Suppose $\widehat{\boldsymbol{\beta}}$ is the estimated parameters obtained from using the bias dataset prepared by over or under-sampling techniques. From Equation (2), the probability that road segment i of cluster j is failed ($y_{ij} = 1$), or survived ($y_{ij} = 0$) becomes,

$$\Pr\left(y_{ij} = 1\right) = \frac{\mathbf{1}}{\mathbf{1}+\boldsymbol{exp}(\boldsymbol{X}_{ij}\widehat{\boldsymbol{\beta}}+\boldsymbol{v}_{j})} \tag{3}$$

where $\widehat{\boldsymbol{\beta}}$ contains β_0 as an estimated intercept.

Next, the prior correction is applied to correct the bias from the bias dataset. This requires the prior knowledge on the fraction of the rare event in the real world. Suppose the proportion of the rare choice in the population as τ and the proportion of the rare choice in the bias dataset is $\bar{y}$. Applying the prior correction method, by leaving other parameters still the same, the correction is applied to the intercept. The corrected intercept, β_0, becomes

$$\beta_0 = \hat{\beta}_0 - \ln\left[\left(\frac{1-\tau}{\tau}\right)\left(\frac{\bar{y}}{1-\bar{y}}\right)\right]. \tag{4}$$

This prior correction method is relatively easy in practice as any logistic regression software can be used for an estimation of the bias parameters and later applying the above correction term at the intercept.

Travel Time Reliability Measurement

The failure model determined from the previous step is used here to measure the reliability of travel time during an extreme event, using the stochastic model as shown in Figure 1. The occurrence of road failure follows the probability function of road segment failure developed in Equation (3), which is determined based on empirical data during the past typhoon. We assume three stages of failures, including moderate, extensive, and completely nonoperational, to determine the different effects on the road segments in each damage stage. Adopting the values used in Haghighi et al *(15)*, the capacity of a link becomes 75% and 50% for moderate and extensive damage respectively. The free flow speed of a link becomes 50% for both moderate and extensive damage. Non-operational links have 0% capacity and free flow speed.

The stochastic failure of the road section is used to determine the capacity of the road system during the typhoon. The daily travel demand, taken from Origin-Destination (OD) matrix of trips, including passenger cars and trucks, were calibrated from observed link traffic counts. Simultaneous failures of road links are generated using Monte Carlo simulation. For each iteration (i.e., for each failure scenario), a random number between 0 and 1 is generated for each link and if it is lower than the calculated failure probability, then we assume the link has failed. If the link fails, another random number between 0 and 1 is generated to randomly assign the failure stage to the failed link. This process is repeated for every link in the road network. According to the generated failure stage, the capacity and free-flow speed of the link are adjusted, while other factors remain the same. Next, the generated road network is input into a traffic assignment model, using the user equilibrium traffic assignment with the standard Bureau of Public Roads (BPR) function for link travel time. In this study, we ran 50 iterations. For every iteration, the results from the traffic assignment are obtained, including link traffic volume, link traverse time, congestion level, link speed, as well as other traffic characteristics. Using the traffic assignment results, a travel time reliability as in *(17, 18)* can be calculated.

RESULTS

The road system of the Tokai region in Japan is selected as a case study. The road network is divided into 100×100 m^2 grid cells. The probability of the failure of each grid cell is determined based on the typhoon rainfall intensity, elevation, land slope, distance to the nearest river and the watershed. The degraded road sections during the 2011 typhoon Roke are obtained from the past government reports, as depicted in Figure 2. The rainfall intensity, as shown in Figure 3, was obtained from the map of 24-hour maximum rainfall in the region during the typhoon.

In fact, many characteristics contribute to a road failure during an extreme event. Such characteristics are, for example, floodplain, runoff patterns, soil and foundation structures. However, they are not easily traceable in practice. Instead, using other spatial geometry of the roads and integrating the spatial correlations among the road segments, the above characteristics that contribute to the risk of road failure can be covered, while the congested roads and the extended impact are modeled through a traffic simulation. Here, we adopted the proximity to the river (see Figure 4 for the maps of river systems) and the elevation of road segments (see Figures 5) and land slope (see Figures 6) and included the spatial correlations among the road sections to explain the failure of a road section during a typhoon. Figure 7 shows the water system of the region in which different watersheds are depicted in different colors. There are 130 watersheds in the region, but only selected watersheds are listed in the legend due to limited space to display all items.

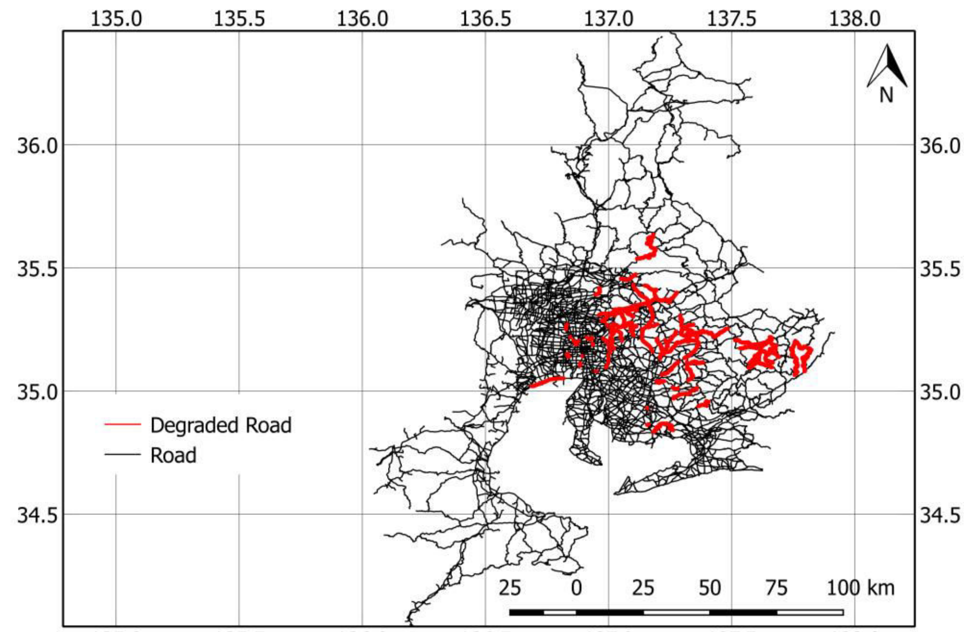

FIGURE 2 Observed degraded links during the 2011 typhoon Roke,

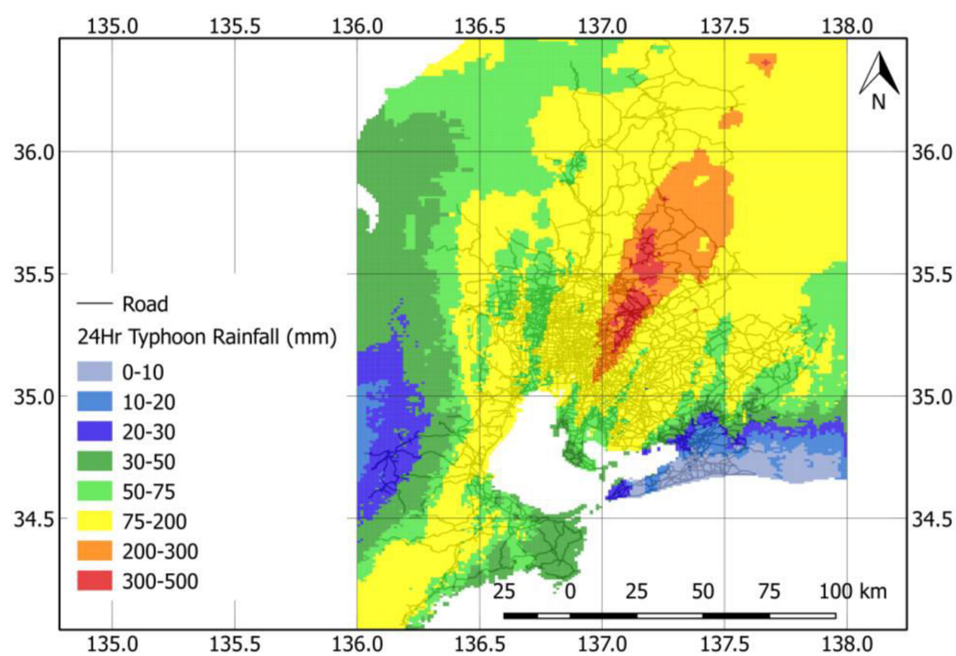

FIGURE 3 24-hour maximum rainfall during the 2011 typhoon Roke (mm)

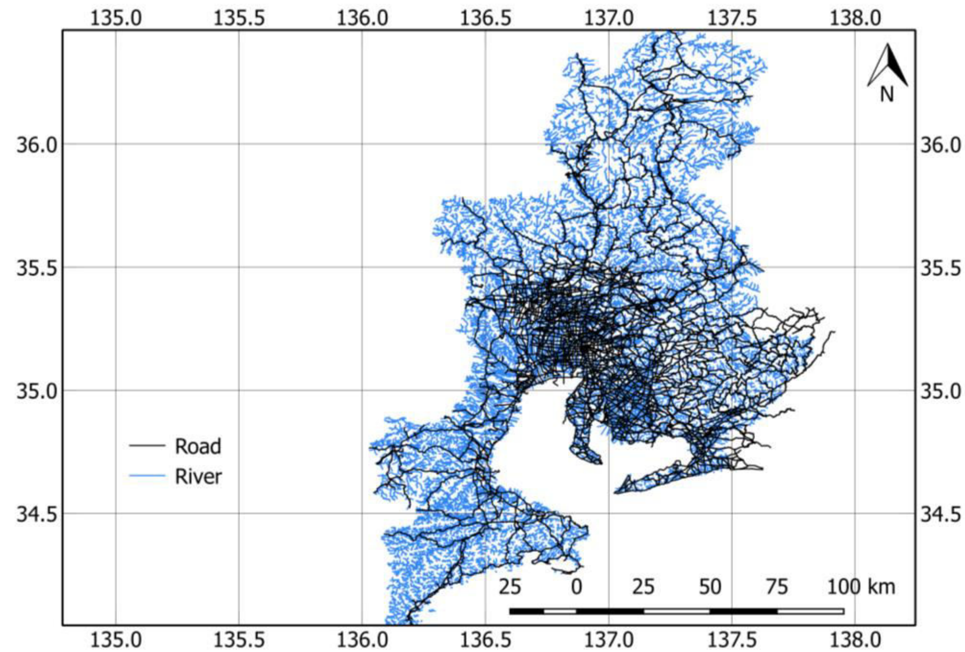

FIGURE 4 Road and river system of the Tokai region

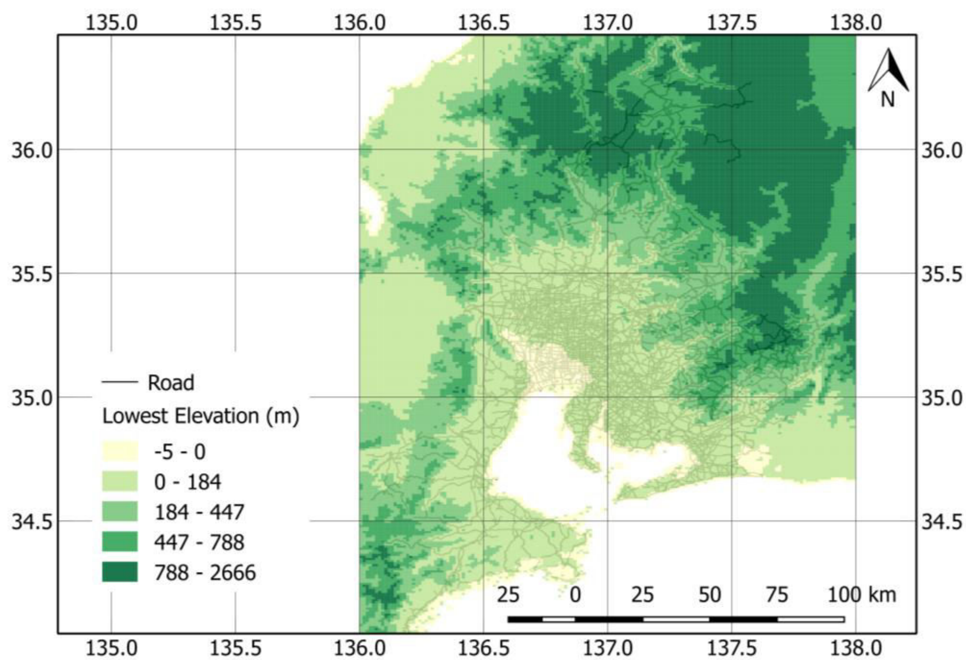

FIGURE 5 Lowest elevation of the Tokai region (m)

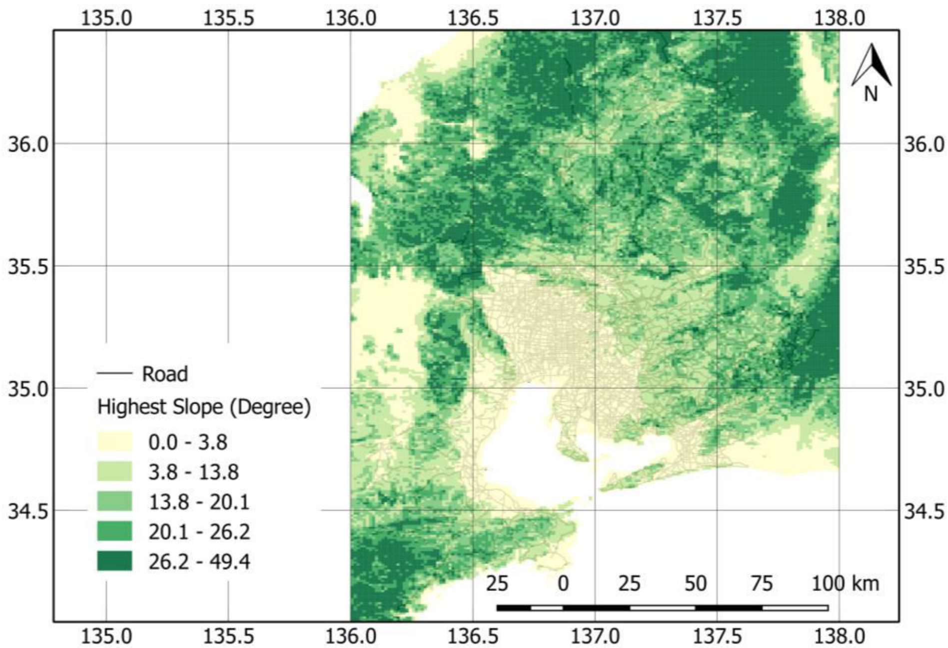

FIGURE 6 Highest land slope of the Tokai region (degree)

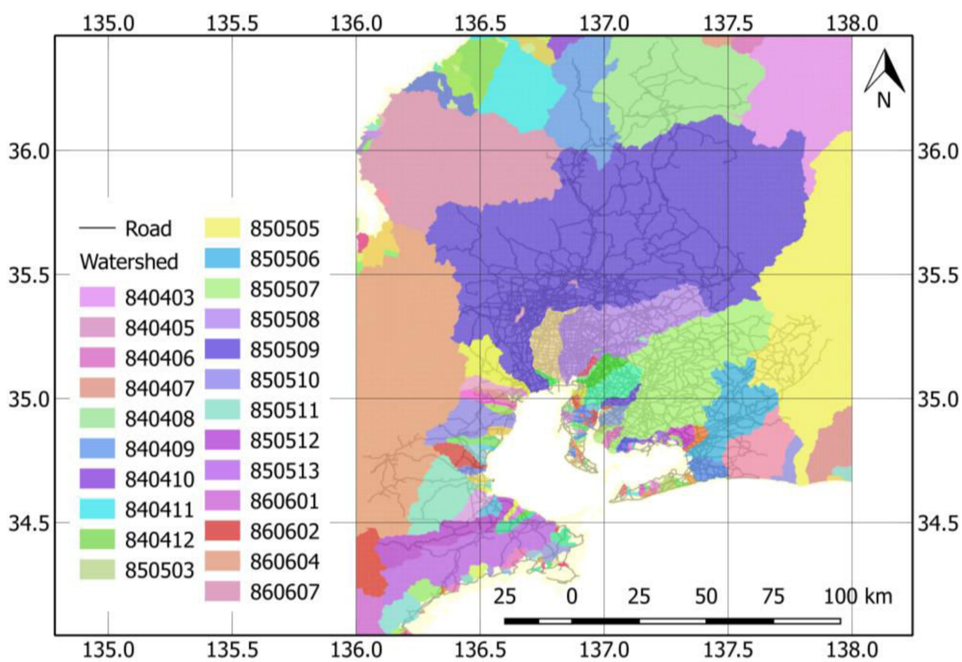

FIGURE 7 Watershed system of the Tokai region
(Not all are presented in the legend. 130 watersheds in total)

The calibration of the failure probability of road segments, as described in the previous section, was performed using MATLAB's tool for Generalized Linear Mixed-Effects Models. Often, although the overall hit ratio is very high in the estimation of a rare event, a general logistic regression can hardly predict the minority. In our case, during the Roke 2011 typhoon 7,446 grids failed and 131,838 grids survived, which is a failure rate of only 5.6%. As explained previously, the method proposed by King and Zeng *(20, 21)*, for improving the predictive accuracy of a rare event, requires a bias dataset with approximately equal numbers for the majority and minority. However, over-sampling technique leads to problems: (1) prone to overfitting problem which is when the model describes the errors instead of the underlying relationship *(26, 27)*, (2) high computational cost during the calibration process since it has to handle an increased number of samples *(28)*. In our case, for a 1:1 over-sampling dataset, we trained 263,676 samples, while we trained only 14,857 samples of a 1:1 under-sampling dataset. Hence, there is a huge reduction in computational cost. Four different proportions between survived and failed grids, including 1:1, 1:2, 1:5 and 1:10 respectively, are prepared using Monte Carlo simulation. These datasets are used to calibrate a binary logistic regression without considering the cluster effect to find the best proportion and best dataset. We generated multiple datasets in each proportion and ones presented here gave the best prediction performance. The results are as shown in Tables 1 and 2 for under-sampling and over-sampling datasets, respectively.

Negative sign of the parameters indicates the tendency to survive and vice versa for the positive parameters. The higher the elevation, the slope and, the intensity of the rainfall, the higher the tendency of the road segment to fail. High elevation and land slope indicate that the road segment is in a mountainous area, where roads are narrow and surrounded by steep slopes and, hence, more vulnerable to failure during a typhoon. The closer the distance to the nearest river, the higher the tendency to fail. Higher precipitation increases the possibility of failure. Hit ratio (00) and hit ratio (11) indicate predictive accuracy of the survived and failed grids (both predicted and observed), respectively. Using the original dataset, although the predictive accuracy of survived grids is very high, only 1.9% of grids are correctly predicted as failed. Clearly, the original dataset strongly underestimates the failure.

Comparing all under-sampling datasets of different proportions, the 1:1 proportion gives the best prediction of the failed grids. Increasing the proportion of the majority worsens the prediction of the minority. Likewise, the 1:1 proportion of over-sampling dataset gives the best prediction comparing with all over-sampling datasets of different proportions. In term of hit ratio, there is no significant difference in the predictive performances of both datasets from 1:1 under and over -sampling, but the number of samples of the under-sampling dataset is 17 times smaller than the over-sampling dataset. There is no benefit in devoting computational effort for the over-sampling dataset, hence we adopt the 1:1 under-sampling dataset for further calculation.

TABLE 1 Calibrated Parameters using Under-sampling Technique at Different Proportions

Parameters	Original Dataset		Under-sampling (1:1)		Under-sampling (1:2)		Under-sampling (1:5)		Under-sampling (1:10)	
	Estimate	t-Stat	Estimate	t-Stat	Estimate	t-Stat	Estimate	t-Stat	Estimate	t-Stat
Intercept	-4.52740	-142.5	-2.14150	-40.7	-2.71210	-61.9	-3.39930	-93.3	-4.01900	-120.6
LowestElevation (m)	0.00031	5.7	0.00069	7.6	0.00054	7.4	0.00039	6.4	0.00033	6.0
HighestSlope (degree)	0.06750	39.1	0.09298	30.0	0.08655	34.3	0.07771	37.9	0.07101	38.6
DistanceToRiver (m)	-0.00045	-12.1	-0.00058	-11.5	-0.00053	-12.0	-0.00050	-12.4	-0.00046	-12.1
24hrTyphoonRainfall(mm)	0.00803	62.7	0.00967	36.5	0.00934	44.6	0.00837	52.7	0.00825	59.5
AIC	51479		16752		23419		34315		43456	
Log Likelihood	-25734		-8370.8		-11704		-17152		-21723	
Number of trained samples	139,284		14,857		22,338		44,676		81,906	
Hit Ratio (00)	0.999		0.715		0.867		0.970		0.994	
Hit Ratio (11)	0.019		0.740		0.369		0.142		0.049	

TABLE 2 Calibrated Parameters using Over-sampling Technique at Different Proportions

Parameters	Original Dataset		Over-sampling (1:1)		Over-sampling (1:2)		Over-sampling (1:5)		Over-sampling (1:10)	
	Estimate	t-Stat	Estimate	t-Stat	Estimate	t-Stat	Estimate	t-Stat	Estimate	t-Stat
Intercept	-4.5274	-142.5	-2.1398	-171.6	-2.6497	-181.0	-3.3879	-175.3	-3.9906	-159.5
LowestElevation (m)	0.00031	5.7	0.0007	30.9	0.0006	22.8	0.0004	12.4	0.0004	8.9
HighestSlope (degree)	0.0675	39.1	0.0901	123.7	0.0824	98.8	0.0734	68.0	0.0682	49.5
DistanceToRiver (m)	-0.00045	-12.1	-0.0005	-45.8	-0.0005	-35.0	-0.0005	-22.9	-0.0005	-16.2
24hrTyphoonRainfall(mm)	0.00803	62.7	0.0098	154.6	0.0090	130.2	0.0085	100.8	0.0082	78.5
AIC	51479		299540		209150		121730		77159	
Log Likelihood	-25734		-149760		-104570		-60862		-38575	
Number of trained samples	139,284		263,676		197,757		158,205		145,021	
Hit Ratio (00)	0.999		0.718		0.873		0.972		0.995	
Hit Ratio (11)	0.019		0.735		0.351		0.143		0.048	

The calibration models with and without the correlation of segments within the same watershed and with and without rare-logit are compared in Table 3. Models 1 and 2 are those presented as the original dataset and the 1:1 under-sampling in Table 1, respectively. Model 3 shows the result of inclusion of the watershed correlation using the original dataset. Model 4 uses the 1:1 under-sampling dataset and considers the watershed correlation. All fixed effect parameters, including intercept, lowest elevation, highest slope, distance to river, and rainfall intensity, are $\boldsymbol{\beta}$ in Equation (2). With the cluster effect, each watershed has its own intercept in addition to the fixed effected intercept for all segments, referring to $\boldsymbol{v}_j$ in the same equation where j indicates watershed j. Since there are 130 watersheds, only selected watersheds are presented in the table. A high t-stat of the watershed intercept indicates a significant correlation of the segments in the watershed.

Considering the quality of the prediction, there is an improvement in log-likelihood and hit ratio (11), when considering the watershed correlation. However, applying both rare-logit estimation together with the cluster effect (Model 4) achieves the best prediction. Taking the average values of the road geometry in Tajimi (Elevation = 135.8 m, Slope = 5.6^{o}, Distance to river = 184.4 m), 113 mm of 24-hour rainfall increases the chance of road failure in Tajimi from 36.8% to 50.0%, when considering the watershed effect.

The calibrated parameters of Models 2 and 4 are used to predict link failures and compare the predictions made with and without the cluster effects applied. Since a road section consists of multiple segments, we assume the road segment having the highest failure probability determines the failure probability of the entire road section. The predicted probability of road failure without and with spatial correlations are depicted in Figures 8 and 9, respectively. Without considering the cluster effects, the shape of the typhoon rainfall intensity outlines the distribution of failure probability. On the other hand, with cluster effects, the distribution of road failure probability is shaped by both the rainfall intensity and the shapes of watershed, which is more aligned with the observed failures shown in Figure 2. Taking the mid-value (138mm) of the yellow area of the 24-hour rainfall map as uniform rainfall, Figure 10 predicts the failure probability when watershed effects are considered. This figure shows that mountainous area in the northeast and the Shonai river basin in the north of Nagoya become vulnerable when the 24-hour rainfall reached 138 mm. It can be interpreted that people living in the Shonai river basin and the mountainous area are likely to experience a travel risk even with moderate typhoon rainfall.

The link failure probabilities are used to measure the travel time reliability using the method described in Figure 1. A random number decides whether a link is affected, and another random number allocates the failure stage of the affected link, which is either moderate, extensive, or completely non-operational. The network used in the traffic assignment is the large-scale road network of the Tokai region, consisting of 6,682 links and 4,218 nodes covering all arterials and expressways in the region. The OD matrix of passenger cars and trucks of 626 zones are input into the traffic assignment.

TABLE 3 Calibrated Parameters for Failure of Road Segment by Typhoon

Parameters	Model 1 w/o Cluster effect & w/o Rare logit		Model 2 w/o Cluster effect & w/ Rare logit		Model 3 w/ Cluster effect & w/o Rare logit		Model 4 w/ Cluster effect & w/ Rare logit	
	Estimate	**t-Stat**	**Estimate**	**t-Stat**	**Estimate**	**t-Stat**	**Estimate**	**t-Stat**
Fixed Effects								
Intercept	-4.52740	-142.5	-2.14150	-40.7	-14.28300	-7.6	-10.96300	-6.5
Lowest Elevation (m)	0.00031	5.7	0.00069	7.6	0.00026	3.6	0.00022	1.7
Highest Slope (degree)	0.06750	39.1	0.09298	30.0	0.09145	38.7	0.07562	17.3
Distance to River (m)	-0.00045	-12.1	-0.00058	-11.5	-0.00077	-22.1	-0.00074	31.3
24hrTyphoonRainfall(mm)	0.00803	62.7	0.00967	36.5	0.00951	51.9	0.01138	-14.1
Cluster Effects (Watershed Intercept)								
…								
Watershed_ID 850507	-	-	-	-	10.594	5.6	9.9459	5.9
Watershed_ID 850508	-	-	-	-	10.011	5.3	9.3615	5.5
Watershed_ID 850509	-	-	-	-	7.5957	4.0	6.8847	4.1
…								
AIC	51479		16752		39431		11493	
Log Likelihood	-25734		-8370.8		-19709		-5740.3	
Hit-Ratio	Predicted = 0	Predicted = 1	Predicted = 0	Predicted = 1	Predicted = 0	Predicted = 1	Predicted = 0	Predicted = 1
Observed = 0	131748	90	94248	37590	131145	693	102471	29367
Observed = 1	7301	145	1936	5510	6560	886	739	6707
Hit Ratio (00)	0.999		0.715		0.995		0.777	
Hit Ratio (11)	0.019		0.740		0.119		0.901	

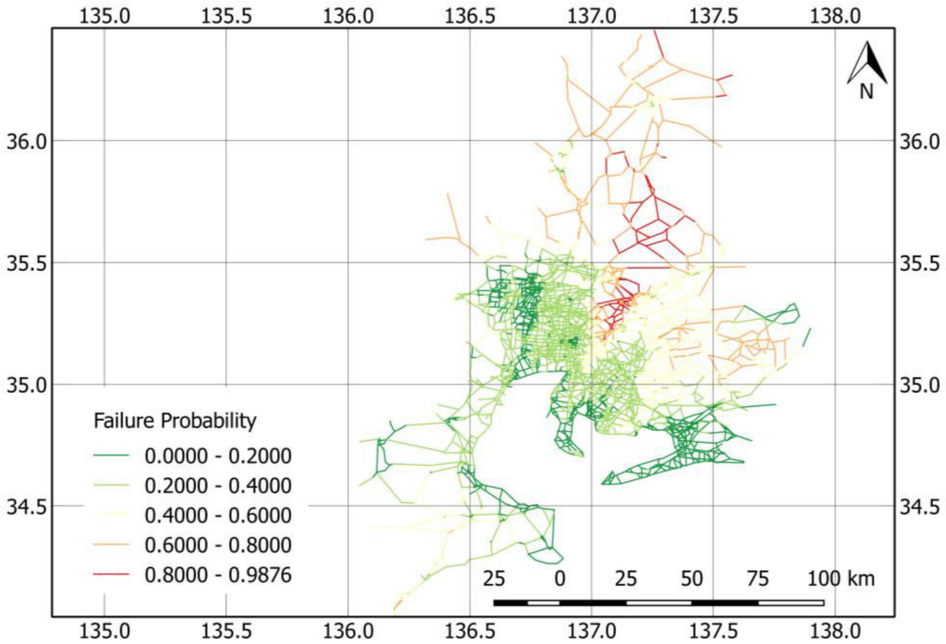

FIGURE 8 Predicted link failures - without cluster effects due to the 2011 typhoon Roke (Model 2)

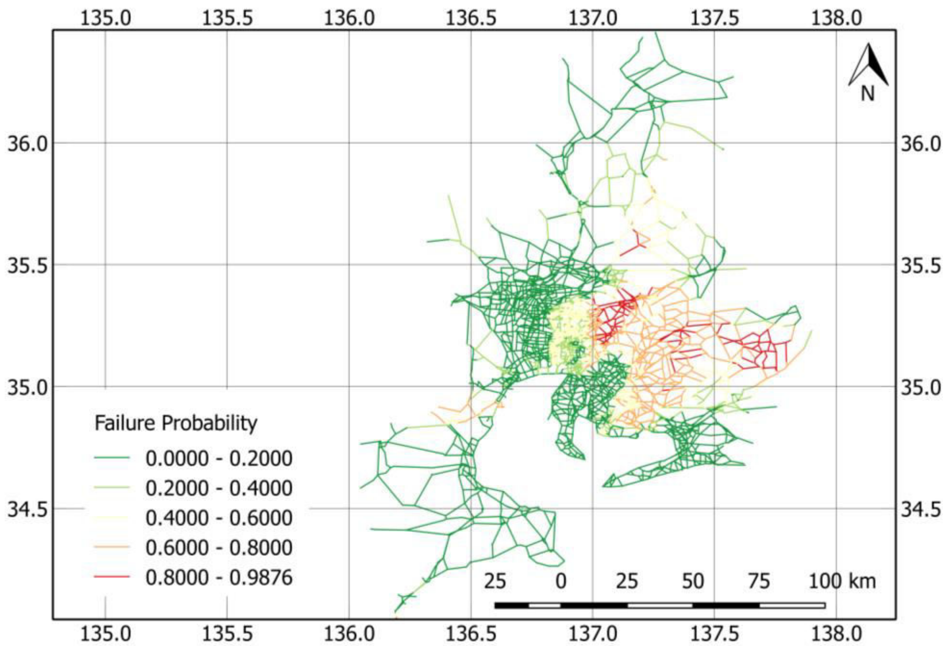

FIGURE 9 Predicted link failures - with cluster effects due to the 2011 typhoon Roke (Model 4)

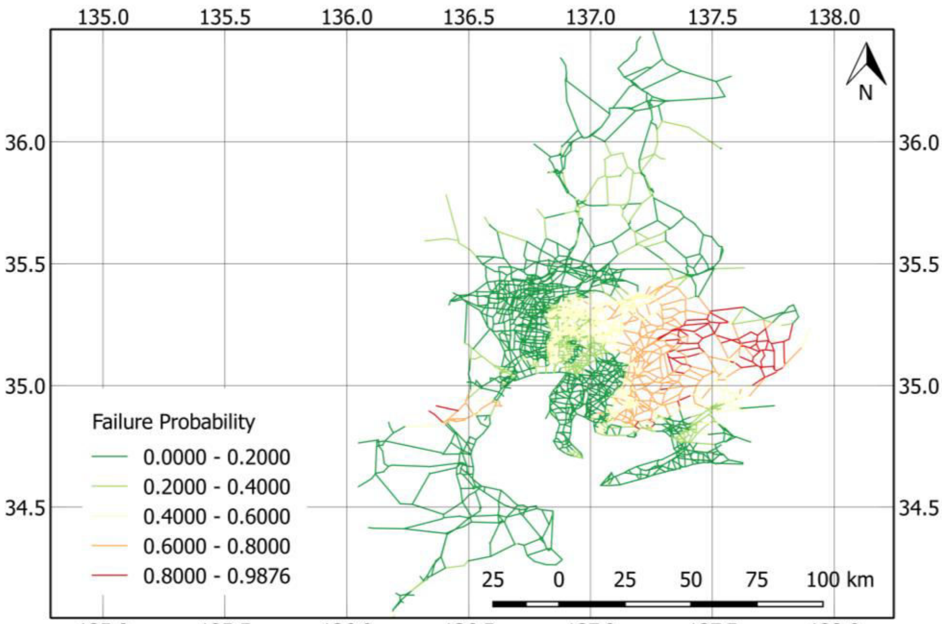

FIGURE 10 Predicted link failures - with cluster effects, assumed a 138 mm 24-hr uniform rainfall

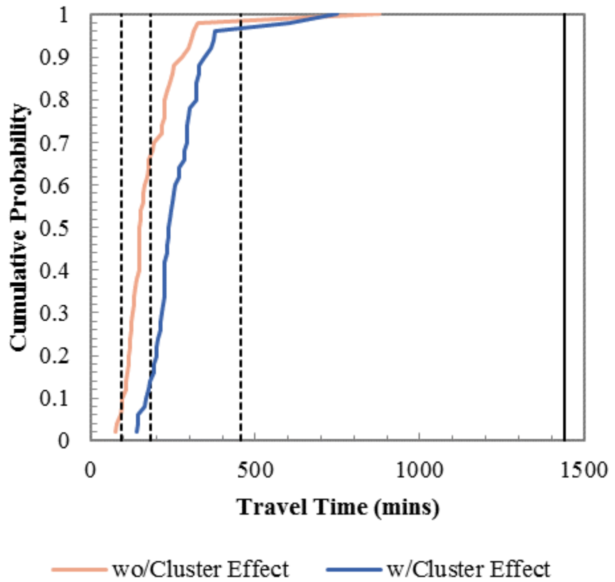

FIGURE 11 Travel time reliability for a trip between Central Nagoya to Tajimi during Typhoon Roke

TABLE 4 Average increase in travel time per vehicle

	Average Increase in Travel Time per Vehicle (Times)	
	All ODs	Nagoya to Tajimi
wo/ Cluster Effect	1.2	4.0
w/ Cluster Effect	2.5	5.8

A trip between central Nagoya and Tajimi is presented here, since trips between this origin and destination were reported as being problematic during the previous typhoon. The cumulative probability of travel time between the OD pairs is shown in Figure 11, with and without cluster effects. This trip typically takes 45.4 minutes under normal conditions. The analysis suggests there is a 67% probability that this trip could take up to 4 times longer (181.7 minutes) in the event of a typhoon, if cluster effects are not considered. If cluster effects are considered the probability reduces to just 14%. We also calculate the average increase in travel time per vehicle of all ODs as shown in Table 4. On average, traveling during the typhoon lengthens the trip duration by 1.2 and 2.5 times, with and without cluster effect, respectively. The duration of a trip between central Nagoya and Tajimi during the typhoon increases, on average, by 4 and 5.8 times, with and without cluster effects, respectively.

CONCLUSION

This paper has presented a method to statistically calculate the failure probability of road segments and the consequent deterioration in travel conditions during an extreme weather event. In previous vulnerability studies, the failure probability was assigned either as a constant failure or a negative exponential distribution. In fact, there are many more factors influencing road failure, especially geometric characteristics. Instead of a probabilistic distribution, this paper estimated the failure probability from empirical data using MELR. However, a normal logistic regression underestimates the failed segments as, in our case, a model using the original dataset can predict only 1.9% of the failed segments correctly. Thus, a rare event logistic regression was applied using an under-sampling technique. We applied a MELR for cluster data to include the spatial correlations among road segments within watersheds. As a result, the model with cluster effects using 1:1 under-sampling dataset provided the best result. The results confirmed that road geometry, including elevation, land slope, and distance to river, were important factors in failure, in addition to the rainfall intensity. Also, the results indicated a strong correlation among failed segments within watersheds. We used the failure probability to determine the impact of the typhoon on travel time reliability and considered three stages of failure: moderate, extensive, and completely non-operational. The results suggested the reliability of travel time between a given OD during the typhoon. Without considering the failure correlations, the travel time reliability might be underestimated. Importantly, this method achieves a better understanding of the failure characteristics as vulnerable links as a group can be identified. For example, authorities can identify regions which are susceptible to typhoons of differing intensities (from high to low) and mitigate accordingly (e.g., putting in place alternative travel options or improving the transport infrastructure) for the most vulnerable regions, potentially reducing the impact of future typhoons.

However, some problems were found during our analysis. The significant watershed intercepts were the only ones affected in the observation. This is because we have data for only one typhoon for the calibration. To improve the quality, we recommend recording information on road failures for a larger set of disasters, preferably in a GIS format to enable onward use. In our case, the failure reports were in the form of text reports and are subject to human error in their interpretation. Particularly, if the records were also to include details of the stage of failure (such as how many lanes of a road were closed), and the timing and duration of failures, the accuracy of the simulation could be improved. Temporal correlations among the failed components could then be performed and, hence, the sequence of failures might be predicted. Such information would give more insight into failure characteristics and inform better road and traffic management strategies (such as locations to install blocks to stop water surge) during an extreme event. In addition, dynamic traffic assignment (e.g., *(29))* or microscopic traffic simulation (e.g., *(30))* can better represent real chaos during an extreme event, although these methods require enormous calculation burden on a large-scale road network. In this study, we considered the 24-hour rainfall along with topographical characteristics of the area to predict the failure probabilities and assumed the road condition was in good condition before the typhoon. However, in fact, there are other factors influencing the failure of the road, such as soil characteristics, basement structure, and the road condition. Hence, an improved calculation can be done to include these characteristics. These issues remain for future work.

ACKNOWLEDGEMENT

This work was developed in collaboration with Thales UK. This support is gratefully acknowledged but implies no endorsement of the findings.

AUTHOR CONTRIBUTION STATEMENT

The authors confirm contribution to the paper as follows: study conception and design: Wisinee Wisetjindawat; data collection: Wisinee Wisetjindawat; analysis and interpretation of results: Wisinee Wisetjindawat; draft manuscript preparation: Wisinee Wisetjindawat, R.Eddie Wilson, Seth Bullock and Alonso Espinosa Mireles de Villafranca.

All authors reviewed the results and approved the final version of the manuscript.

REFERENCES

1. Taylor M. *Vulnerability Analysis for Transportation Networks*, Elsevier, Cambridge, 2017.
2. Chen, X.Z, Q.C. Lu, Z.R. Peng, and J.E. Ash. Analysis of Transportation Network Vulnerability under Flooding Disaster. *Transportation Research Record: Journal of the Transportation Research Board*, 2015. 2532: 37-44.
3. Lauthep, P. *Stochastic Transport Network Model and Optimization for Reliability and Vulnerability Analysis*, Doctoral Thesis, The Hong Kong Polytechnic University, 2011.
4. Amini, B., F. Peiravian, M. Mojarraadi, and S. Derrible. Comparative Analysis of Traffic Performance of Urban Transportation Systems. *Transportation Research Record: Journal of the Transportation Research Board*, 2016. 2594: 159-168.
5. Iida, Y., and H. Wakabayashi. An Approximation Method of Terminal Reliability of a Road Network Using Partial Minimal Path and Cut Set. *Presented at 5th World Conference of Transport Research*, Yokohama, 1989.
6. Chen, A., H. Yang, H.K. Lo, and W.H. Tang. Capacity Reliability of a Road Network: an Assessment Methodology and Numerical Results. *Transportation Research Part B*, 2002. 36: 225-252.
7. Asakura, Y. Reliability Measures of an Origin and Destination Pair in a Deteriorated Road Network with Variable Flows. *Presented at 4th Meeting of the EURO Working Group in Transportation*, 1996.
8. Chen A., H. Yang, H.K. Lo, and W.A. Tang. Capacity Related Reliability for Transportation Networks. *Journal of Advanced Transportation*, 1999. 33(2): 183-200.
9. Kermanshah, A., and S. Derrible. A Geographical and Multi-Criteria Vulnerability Assessment of Transportation Networks against Extreme Earthquakes. *Reliability Engineering & System Safety*, 2016. 153: 39-49.
10. Berch, B., C. von Ferber, T. Holovatch, and Y. Holovatch. Resilience of Public Transport Networks against Attacks. *The European Physical Journal B*, 2009. 71: 125-137.
11. Jenelius, E., T. Petersen, and L.G. Mattsson. Importance and Exposure in Road Network Vulnerability Analysis. *Transportation Research Part A*, 2006. 40: 537-560.
12. Taylor, M., S. Sekhar, and G. D'Este. Application of Accessibility Based Methods for Vulnerability Analysis of Strategic Road Networks. *Network and Spatial Economics*, 2006. 6(3-4): 267-291.
13. Taylor, M. Critical Transport Infrastructure in Urban Areas: Impacts of Traffic Incidents Assessed using Accessibility-Based Network Vulnerability Analysis. *Growth and Change*, 2008. 39(4): 593-616.
14. Sumalee, A., and F. Kurauchi. Network Capacity Reliability Analysis Considering Traffic Regulation after a Major Disaster. *Network Spatial Economics*, 2006. 6: 205-219.

15. Haghighi, N., K. Fayyaz, X. Liu, and S. Bartlett. Identifying Network-wide Critical Transportation Links under Disaster Disruptions: A Multi-Scenario and Probability-Based Simulation Approach. *Presented at 96th Transportation Research Board Annual Meeting*, Washington, D.C., 2017.
16. Asadabadi, A, and Miller-Hooks E. Optiomal Transportation and Shoreline Investiment Planning under a Stochastic Climate Future. *Transportation Research Part B*, 2017, 100: 156-174.
17. Wisetjindawat, W., A. Kermanshah, S. Derrible, and M. Fujita. Stochastic Modeling of Road System Performance during Multihazard Events: Flash Floods, and Earthquakes, *Journal of Infrastructure Systems*, 2017. 23(4).
18. Wisetjindawat, W., S. Derrible, and A. Kermanshah. Modeling the Effectiveness of Infrastructure and Travel Demand Management Measures to Improve Traffic Congestion During Typhoons, *Transportation Research Record,* 2018.
19. Guns M. and V. Vanacker. Logistic Regression Applied to Natural Hazards: Rare Event Logistic Regression with Replications. *Natural Hazards Earth System Sciences*, 2012. 12: 1937-1947.
20. King G. and L. Zeng. Logistic Regression in Rare Events Data. *The Society for Political Methodology*, 2001. 9(2): 137-163.
21. King G. and L. Zeng. Explaining Rare Events in International Relations. *International Organization*, 2001. 55(3): 693-715.
22. Bai, S., G. Lu, J. Wang, P. Zhou, and L. Ding. GIS-based Rare Events Logistics Regression for Landslide-Susceptibility Mapping of Lianyungan, China. *Environmental Earth Science*, 2011. 62: 139-149.
23. Ten Have, T., A. Kunselman, L. Tran. A Comparison of Mixed Effects Logistic Regression Models for Binary Response Data with Two Nested Levels of Clustering. *Statistics in Medicine*, 1999. 18(8): 947-60.
24. Bhat, C., and J. Guo. A Mixed Spatially Correlated Logit Model: Formulation and Application to Residential Choice Modelling. *Transportation Research Part B*, 2004. 38(2): 147-168.
25. Vermunt, J. Mixed-Effects Logistic Regression Models for Indirectly Observed Discrete Outcome Variables. *Multivariate Behavioral Research*, 2005. 40(3): 281-301.
26. Chawla, N.V. Data Mining for Imbalanced Datasets: An Overview In: *Data Mining and Knowledge Discovery Handbook (*Maimon, O. and L. Rokach, ed.), Springer, 2010, pp. 875-886.
27. Lui, A.Y. The Effect of Oversampling and Undersampling on Classifying Imbalanced Text Datasets. Graduation Thesis, University of Texas at Austin, 2004.

28. Ertekin, S. Adaptive Oversampling for Imbalanced Data Classification. In: Gelenbe E., Lent R. (eds) Information Sciences and Systems 2013. *Lecture Notes in Electrical Engineering*, Vol. 264. Springer, Cham, 2013.
29. Du, L., G. Song, Y. Wang, J. Huang, M. Ruan, and Z. Yu. Traffic Events Oriented Dynamic Traffic Assignment Model for Expressway Network: A Network Flow Approach. *IEEE Intelligent Transportation Systems Magazine*, 2018. 10(1): 107-120.
30. Samoili, S., A. Bhaskar, M.H. Pham, M.H., and A. Dumont. Considering weather in simulating traffic. *Presented at the 11th Swiss Transport Research Conference*, Monte Verita, Ascona, 2011.